Inorganic Chemistry

Article

pubs.acs.org/IC

Luminescent Mechanochromism in a Gold(I)−Copper(I) N-Heterocyclic Carbene Complex

Kelly Chen, Michelle M. Nenzel, Thomas M. Brown, and Vincent J. Catalano*

Department of Chemistry, University of Nevada, Reno, Nevada 89557, United States

Supporting Information

ABSTRACT: The silver(I) species $[Ag(benzim(CH_2py)_2)_2]PF_6$ (**1**) was prepared by refluxing the ligand precursor $[H(benzim(CH_2py)_2)_2]PF_6$ with Ag_2O and aqueous sodium hydroxide in dichloromethane. Simple transmetalation of **1** with tetrahydrothiophenegold(I) chloride forms the gold(I) analogue $[Au(benzim(CH_2py)_2)_2]PF_6$ (**2**). The addition of 2 equiv of $[Cu(NCCH_3)_4]PF_6$ to **2** in acetonitrile produces a blue-luminescent, trimetallic complex, $[AuCu_2(benzim(CH_2py)_2)_2(NCCH_3)_4](PF_6)_3{\cdot}2CH_3CN$ (**3**·2CH_3CN). When blue-luminescent **3**·2CH_3CN is exposed to air, the complex loses four acetonitrile molecules, and the emission of the desolvated complex (**4**) appears aquamarine. Crystallization of **4** from different solvents produces the complexes $[AuCu_2(benzim(CH_2py)_2)_2](PF_6)_3$ (**5**) and $[AuCu_2(benzim(CH_2py)_2)_2(NCCH_2CH_3)_2](PF_6)_3$ (**6**). Upon grinding, both **3**·2CH_3CN and **4** exhibit mechanochromic transformations to a yellow-luminescent powder (*ground*-**4**). The reversible mechanochromic transformation of **3**·2CH_3CN to *ground*-**4** is a crystalline-to-amorphous conversion accompanied by partial desolvation. The luminescent mechanochromism of **4** to *ground*-**4** is an "amorphous-to-amorphous" process and does not require solvent loss. In addition to their mechanochromic properties, both **3**·2CH_3CN and **4** exhibit luminescent thermochromism through desolvation to form a weak luminescent powder (**7**).

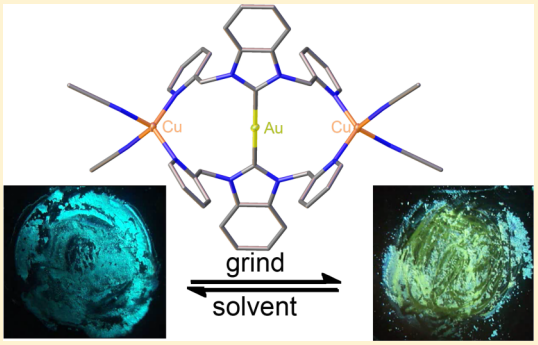

INTRODUCTION

Mechanochromism is the change of color of a compound upon the addition of mechanical stimuli, typically grinding. This process is usually reversible upon the application of solvent, vapor, or heat.[1] Mechanochromism is seen in many organic molecules, polymers,[2,3] and, to a lesser extent, metal complexes.[4−25] The unground and ground forms tend to have different molecular arrangements and intermolecular interactions, leading to different optical properties. Mechanochromic transformations are often categorized into two groups: those with distinct phase transitions (i.e., single crystal to single crystal)[4,5,7,8,26−28] and those involving conversion from a crystalline phase to an amorphous state.[6,9−14,17,20,22]

Recently, Ito and co-workers reported the remarkable single-crystal-to-single-crystal transformation of phenyl(3,5-dimethylphenylisocyanide)gold.[7] Mechanical picking of a section of the crystal with a needle produces a phase transition that spreads throughout the crystal and changes the emission from bright green to weak blue. Using single-crystal X-ray diffraction, they determined that the differences in emission in the two crystals were due to changes in the strength of aurophilic and $\pi-\pi$/CH$-\pi$ interactions. In addition to metallophilic and $\pi-\pi$ intermolecular interactions, mechanochromic transformations are also influenced by the solvent. In 2010, Tzeng and co-workers studied the mechanochromism of zinc metal−organic frameworks (MOFs).[5] The crystal structure of the green-luminescent compound $\{[ZnL_2(H_2O)_2](ClO_4)_2\}_n$ contained two water molecules coordinated to the zinc(II) center. Upon exposure to air, the MOF desolvates, and the two ClO_4^- anions coordinate instead. When the desolvated blue-luminescent solid is ground in the presence of moisture, the MOF reverts back to the original water-coordinated, green-luminescent form. In 2012, Chen and co-workers reported the mechanochromism of several platinum(II) compounds and their solvates.[14] Upon grinding, the solvates lose their lattice solvents to form amorphous solids. However, solvent loss was not a requirement for mechanochromic transformation. Surprisingly, a grinding-induced crystalline-to-amorphous transformation also occurred in the desolvated species.

Previously, we reported the vapochromic properties of a luminescent gold(I)−copper(I) N-heterocyclic carbene (NHC) complex, $[AuCu_2(im(CH_2py)_2)_2(NCCH_3)_4](PF_6)_3$, that responds to solvent vapor, in particular methanol.[29] Exposing solid samples of blue-luminescent $[AuCu_2(im(CH_2py)_2)_2(NCCH_3)_4](PF_6)_3$ to methanol vapor produces bright-green-luminescent $[AuCu_2(im(CH_2py)_2)_2(CH_3OH)_2](PF_6)_3$, where the four coordinated acetonitrile molecules are replaced with two methanol ligands along with a significant molecular reorganization. The long gold(I)−copper(I) separations (~4.6 Å) in $[AuCu_2(im(CH_2py)_2)_2(NCCH_3)_4](PF_6)_3$ are shortened to ~2.7 Å in $[AuCu_2(im(CH_2py)_2)_2(CH_3OH)_2]$-

Received: April 10, 2015
Published: July 8, 2015

DOI: 10.1021/acs.inorgchem.5b00821
Inorg. Chem. 2015, 54, 6900−6909

Scheme 1. Preparation of 3·2CH$_3$CN

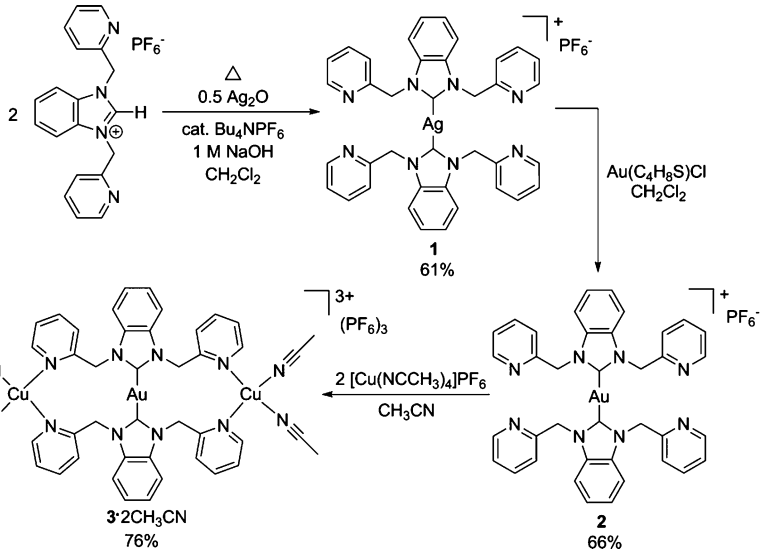

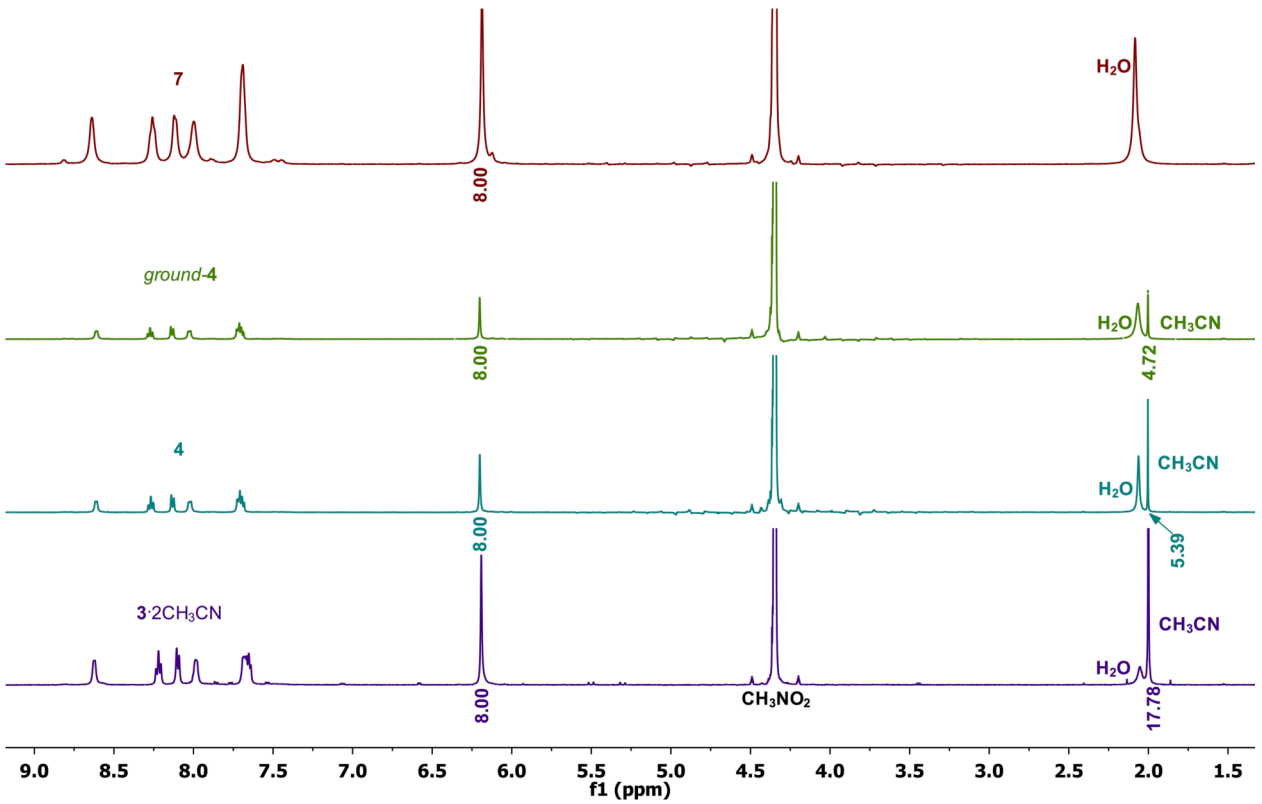

Figure 1. ^{1}H NMR (500 MHz, CD_3NO_2) spectra of **3**·2CH$_3$CN, **4**, *ground*-**4**, and **7**.

$(PF_6)_3$. These complexes are robust, and this process is highly reversible. We questioned whether other gold−copper NHCs would exhibit similar vapochromic properties. Although we have yet to find a similarly dramatic vapochromic response to solvent, we have discovered an unusual luminescent mechanochromic transformation in an analogous benzimidazole-substituted gold(I)−copper(I) NHC complex.

RESULTS

As shown in Scheme 1, $[AuCu_2(benzim(CH_2py)_2)_2(NCCH_3)_4](PF_6)_3{\cdot}2CH_3CN$ (**3**·2CH$_3$CN) was prepared analogously to the previously reported $[AuCu(im(CH_2py)_2)_2(NCCH_3)_4](PF_6)_3{\cdot}2CH_3CN$ complex.[29] The silver(I) NHC complex $[Ag(benzim(CH_2py)_2)_2]PF_6$ (**1**) was prepared with difficulty by the addition of Ag_2O and 1 M NaOH to a dichloromethane solution of $[H(benzim(CH_2py)_2)_2]PF_6$ and a catalytic amount of Bu_4NPF_6 followed by refluxing for several hours. A major issue with the synthesis is the inadvertent formation of the triangular $[Ag_3(NHC)_3]^{3+}$ species previously reported by Chen and co-workers.[30] Transmetalation of **1** with tetrahydrothiophenegold(I) chloride produces the homoleptic gold(I) species $[Au(benzim(CH_2py)_2)_2]PF_6$ (**2**). The addition of 2 equiv of $[Cu(NCCH_3)_4]PF_6$ to **2** in acetonitrile generates the gold(I)−

DOI: 10.1021/acs.inorgchem.5b00821
Inorg. Chem. 2015, 54, 6900−6909

Table 1. X-ray Crystallographic Data for 2, 3·2CH$_3$CN, 5, and 6

	2	3·2CH$_3$CN	5	6
formula	$C_{38}H_{32}AuF_6N_8P$	$C_{50}H_{50}AuCu_2F_{18}N_{14}P_3$	$C_{83}H_{64}Au_2Cu_4F_{36}N_{23}O_{14}P_6$	$C_{46}H_{48}AuCu_2F_{18}N_{12}O_4P_3$
fw	942.65	1605.99	3125.48	1591.92
temperature, K	100(2)	100(2)	100(2)	100(2)
cryst size, mm^3	0.248 × 0.055 × 0.043	0.10 × 0.08 × 0.08	0.498 × 0.086 × 0.082	0.126 × 0.030 × 0.030
cryst syst	triclinic	monoclinic	triclinic	triclinic
space group	$P\bar{1}$	$P2_1/n$	$P\bar{1}$	$P\bar{1}$
a, Å	8.1963(3)	9.2370(8)	17.5182(9)	8.1559(6)
b, Å	10.3998(4)	25.546(2)	18.7146(9)	12.6903(9)
c, Å	11.8265(5)	12.8114(11)	19.0445(9)	13.6732(9)
α, deg	68.4320(10)	90	73.9785(8)	81.8321(14)
β, deg	88.3480(10)	96.4654(15)	63.6056(8)	84.8442(13)
γ, deg	70.5250(10)	90	79.8442(9)	76.6665(13)
V, Å^3	878.80(6)	3003.9(4)	5365.1(5)	1360.67(17)
Z	1	2	2	1
ρ, Mg·m^{-3}	1.781	1.776	1.935	1.943
μ, mm^{-1}	4.305	3.322	3.725	3.670
reflns collected	20351	57765	112966	25645
indep reflns	4657 [R(int) = 0.0469]	7958 [R(int) = 0.0460]	24649 [R(int) = 0.0561]	5370 [R(int) = 0.1078]
completeness to θ = 25.242°, %	100.0	100.0	100.0	100.0
R1, wR2 [$I > 2\sigma(I)$]	0.0257, 0.0546	0.0271, 0.0568	0.0355, 0.0837	0.0460, 0.0800

copper(I) species 3·2CH$_3$CN in modest yields. Compounds **1**, **2**, and 3·2CH$_3$CN have limited solubility in chlorinated solvents but are readily soluble in nitriles. All of these compounds are air-stable in both the solution and solid states.

Compounds **1**, **2**, and 3·2CH$_3$CN were characterized by ^{1}H and ^{13}C{^{1}H} NMR spectroscopy. NMR spectra of [H(benzim-(CH$_2$py)$_2$)$_2$]PF$_6$, **1**, and **2** are presented in Figures S1−S6 in the Supporting Information (SI). The ^{1}H NMR spectrum of **1** is similar to that of the ligand precursor [H(benzim-(CH$_2$py)$_2$)]PF$_6$.[30] The ^{1}H NMR spectrum of the ligand precursor in (CD$_3$)$_2$CO contains a singlet at 6.01 ppm corresponding to the methylene protons, with several multiplets in the aromatic region from 7.26 to 8.50 ppm. Additionally, a singlet corresponding to the proton on the carbenic carbon appears at 11.82 ppm. The addition of Ag$_2$O to the ligand precursor to form **1** eliminates this resonance. A similar change is observed in the ^{13}C{^{1}H} NMR spectrum of **1**, which lacks the peak corresponding to the carbenic carbon. The NMR spectra of **1** and gold-containing **2** are also similar. However, the ^{1}H NMR spectrum of **1** in (CD$_3$)$_2$CO features two multiplets at 7.44 and 7.51 ppm, although these analogous peaks coalesce in the spectrum of **2**. The ^{13}C{^{1}H} NMR spectrum of **2** is similar to that of **1** but contains a peak at 193.3 ppm corresponding to the carbenic carbon.

As shown in Figure 1, the ^{1}H NMR spectrum of 3·2CH$_3$CN in CD$_3$NO$_2$ features a singlet at 6.19 ppm corresponding to the methylene protons of the ligands and several multiplets from 7.65 to 8.22 ppm. Furthest downfield, a singlet also appears at 8.60 ppm assigned to the protons adjacent to the nitrogen atoms of the pyridyl groups. Upfield, a resonance that integrates to ∼18 protons is found at 2.00 ppm, corresponding to six acetonitrile molecules. In CD$_3$NO$_2$, free acetonitrile also resonates at 2.00 ppm, suggesting that the coordinated acetonitrile ligands in 3·2CH$_3$CN dissociate from the copper(I) center in solution. Full ^{1}H and ^{13}C{^{1}H} NMR spectra of 3·2CH$_3$CN are presented in Figures S7−S9 in the SI.

Compounds **2** and 3·2CH$_3$CN were also characterized by single-crystal X-ray diffraction. Crystallographic data for all crystal structures are summarized in Table 1, and full bond lengths and angles for all crystal structures are presented in Tables S1−S12 in the SI. Blue-luminescent crystals of **2** were obtained by vapor diffusion of diethyl ether into an acetonitrile solution of **2**. Compound **2** crystallizes in the $P\bar{1}$ space group, with half of the molecule occupying the asymmetric unit and the other half generated through an inversion operation. As shown in Figure 2, the compound features a gold(I) ion linearly bonded to the two NHC ligands, with the benzimidazolylidene rings rigorously coplanar to one another. The Au1−C1 distance of 2.013(3) Å is typical for gold NHC complexes.[31] Selected bond distances and angles of **2** are listed in Table 2.

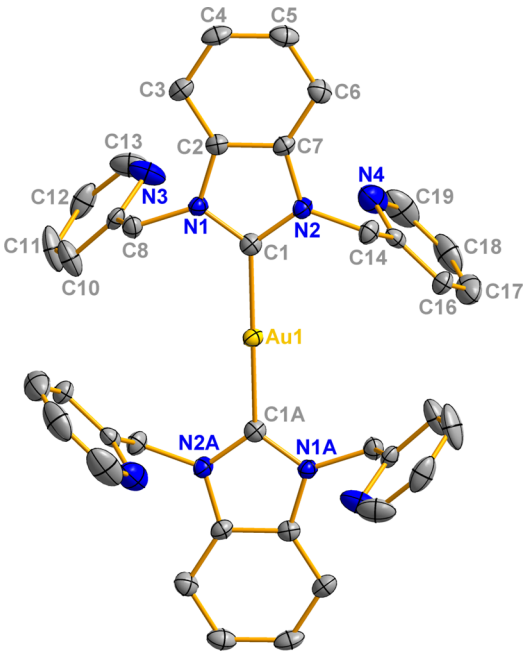

Figure 2. Thermal ellipsoid plot (50%) of the cationic portion of **2**. Hydrogen atoms are omitted for clarity. The atoms labeled with A are generated through inversion.

DOI: 10.1021/acs.inorgchem.5b00821
Inorg. Chem. 2015, 54, 6900−6909

Table 2. Selected Bond Distances (Å) and Angles (deg) of 2

Au1−C1	2.013(3)	C1−Au1−C1A	180.00(6)
C1−N1	1.351(3)	Au1−C1−N1	127.83(19)
C1−N2	1.347(3)	Au1−C1−N2	125.63(19)
C2−N1	1.393(3)	N1−C1−N2	106.5(2)
C8−N1	1.462(3)	C1−N1−C2	110.3(2)
C7−N2	1.391(3)	C1−N2−C7	110.9(2)
C14−N2	1.464(3)	C1−N1−C8	123.6(2)
C2−C7	1.389(4)	C1−N2−C14	123.4(2)

Blue-luminescent crystals of **3**·2CH_3CN were grown by vapor diffusion of diethyl ether into an acetonitrile solution of **3**·2CH_3CN. Compound **3**·2CH_3CN crystallizes in the $P2_1/n$ space group, with half of the molecule occupying the asymmetric unit and the gold(I) center residing on an inversion center. Selected bond distances and angles are listed in Table 3.

Table 3. Selected Bond Distances (Å) and Angles (deg) for 3·2CH_3CN

Au1···Cu1	4.6239(5)	Cu1−Au1−Cu1A	180.0
Au1−C1	2.014(2)	N4−Cu1−N5	106.84(8)
Cu1−N4	2.0285(19)	N4−Cu1−N6	113.42(8)
Cu1−N5	2.023(2)	N5−Cu1−N6	99.66(9)
Cu1−N6	2.009(2)	N4−Cu1−N3A	118.57(7)
C1−N1	1.354(3)	N5−Cu1−N3A	105.61(9)
C1−N2	1.350(3)	N6−Cu1−N3A	110.57(8)
C8−N1	1.466(3)	Au1−C1−N1	126.99(18)
C14−N2	1.470(3)	Au1−C1−N2	126.51(17)
		N1−C1−N2	106.5(2)

The structure is similar to that of the previously reported $[AuCu_2(im(CH_2py)_2)_2(NCCH_3)_4](PF_6)_3$·2$CH_3CN$.[29] As shown in Figure 3, the complex features a central gold(I) ion

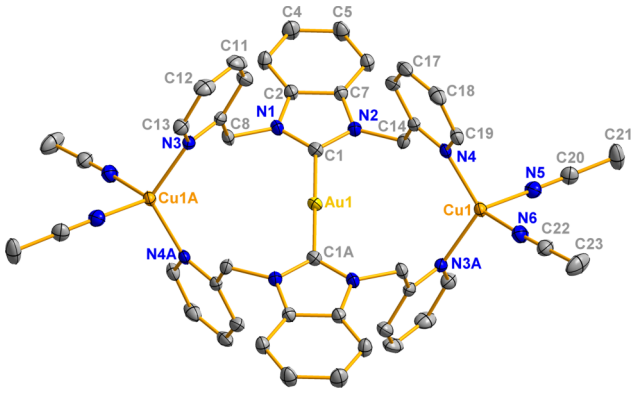

Figure 3. Thermal ellipsoid (50%) plot of the cationic portion of **3**·2CH_3CN. Hydrogen atoms are excluded for clarity. The atoms labeled with A are generated through inversion.

linearly bonded to two NHC ligands through two flanking copper(I) ions coordinated to the pyridyl groups. Each copper center is further bonded to two acetonitrile ligands to form a distorted tetrahedral geometry, and two additional acetonitrile solvate molecules occupy the lattice. The pyridyl rings of the same NHC ligand are bent away from each other and toward each copper(I) ion. These pyridyl rings occupy one face of the complex, while the pyridyl rings from the second NHC are oriented toward the opposite face. The metal centers are isolated from one another with a long Au1···Cu1 distance of 4.6239(5) Å. Because of the crystallographic symmetry in **3**·2CH_3CN, the Cu1−Au1−Cu1A angle is exactly 180°, and the benzimidazolylidene rings are rigorously coplanar. The copper centers adopt a pseudotetrahedral geometry, with N−Cu−N angles ranging from 99.66(9) to 118.57(7)°. The Cu−N distances range from 2.009(2) to 2.0285(19) Å.

Compounds **1**, **2**, and **3**·2CH_3CN are colorless solids. In acetonitrile, all three complexes have absorption bands below 300 nm, similar to those of the ligand precursor. Under UV illumination, both **1** and **2** emit bright blue in acetonitrile with broad emission bands at 448 and 455 nm, respectively. In the solid state, the emission of **2** intensifies and red-shifts to 485 nm. Optical spectra of **1**, **2**, and **3**·2CH_3CN are presented in Figures S10−S16 in the SI. The trimetallic **3**·2CH_3CN is weakly emissive in solution (Figure S16 in the SI) but is intensely emissive in the solid state with a relatively narrow band at 461 nm (λ_{ex}= 365 nm; Figure 4).

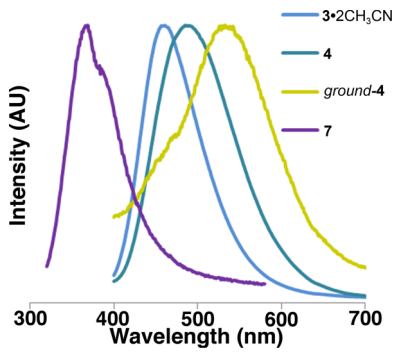

Figure 4. Normalized solid-state emission of **3**·2CH_3CN, **4**, *ground*-**4**, and **7** (λ_{ex} = 365 nm for **3**, **4**, and *ground*-**4** and 300 nm for **7**).

Upon prolonged exposure to air (>1.5 h), both crystalline and powder forms of **3**·2CH_3CN desolvate to form **4** (Scheme 2), and the blue emission (λ_{max} = 461 nm) shifts to a bright aquamarine (λ_{max} = 485 nm; Figure S17 in the SI). As shown in Figure 1, the ^{1}H NMR spectrum of **4** in CD_3NO_2 is nearly identical with that of **3**·2CH_3CN, except only two acetonitrile molecules are present. On the basis of the NMR spectrum, it is unclear whether these solvents occupy the lattice or remain coordinated to the copper centers. Complete ^{1}H and $^{13}C\{^1H\}$ NMR spectra of **4** are presented in Figures S18 and S19 in the SI. However, the solid-state ATR-IR spectrum of **4** contains a weak band at 2271 cm^{-1} assigned to ν(CN). This is very close in energy to that observed for a solid sample of $[Cu(CH_3CN)_4]PF_6$, where the ν(CN) band appears at 2273 cm^{-1}. For comparison, the ATR-IR spectrum of **3**·2CH_3CN shows a ν(CN) band at 2279 cm^{-1} along with a sharper band at 2253 cm^{-1}, which is identical with that of a liquid acetonitrile solvent. ATR-IR spectra are presented in the SI (Figure S20). Recrystallization of **4** from acetonitrile regenerates the blue-emissive **3**·2CH_3CN material. Desolvation is also observed in the gas phase; the high-resolution positive-ion electrospray ionization (ESI^+) mass spectrometry (MS) spectrum of **3**·2CH_3CN exclusively produced isotope patterns consistent with those of $[AuCu_2L_2(PF_6)_2]^+$. High-resolution MS spectra of $[H(benzim(CH_2py)_2)_2]PF_6$, **2**, and **3**·2$CH_3CN$ are presented in Figures S21−S23 in the SI.

Numerous attempts to crystallize **4** from a noncoordinating solvent such as nitromethane consistently produced green-luminescent crystals of an acetonitrile-free material identified as

DOI: 10.1021/acs.inorgchem.5b00821
Inorg. Chem. 2015, 54, 6900−6909

Scheme 2. Luminescent Mechanochromism and Thermochromism of 3·2CH$_3$CN and 4[a]

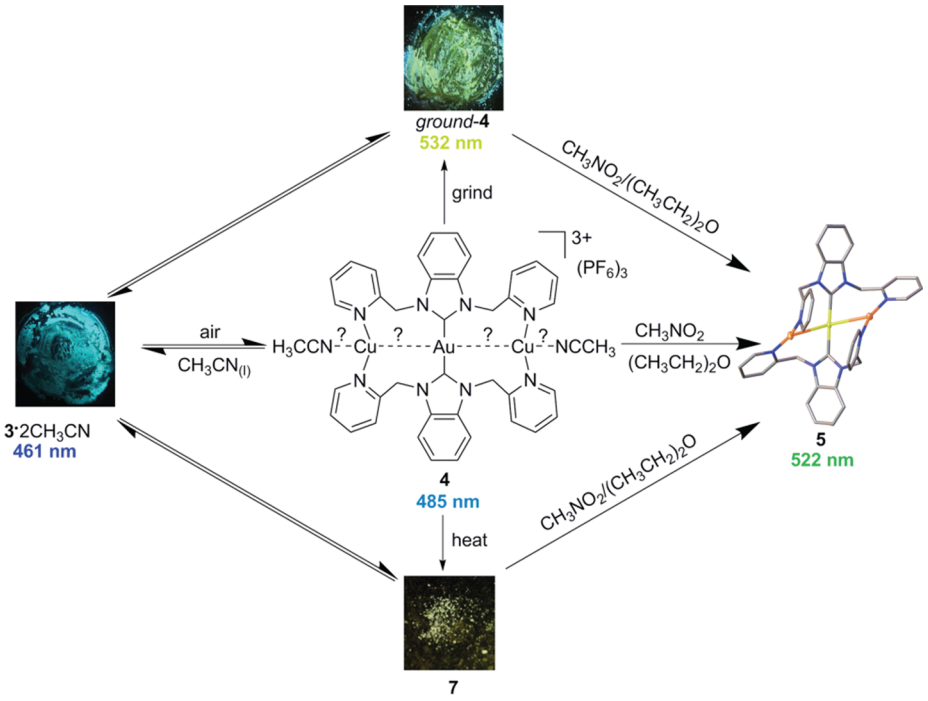

[a]Inset photographs: powders of 3·2CH$_3$CN, *ground*-**4**, and **7** under 365 nm illumination.

Scheme 3. Attempted Crystallization of 4 To Produce 5 and 6

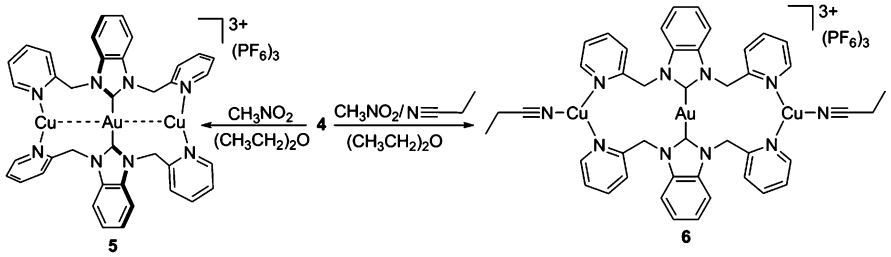

$[AuCu_2(benzim(CH_2py)_2)_2](PF_6)_3$ (**5**; Scheme 3). X-ray-quality crystals of **5** were obtained by vapor diffusion of diethyl ether into a purified nitromethane solution of **4**. Compound **5** crystallizes in the $P\bar{1}$ space group. There are two $[AuCu_2(NHC)_2]^{3+}$ cations in the asymmetric unit. One is shown in Figure 5, but both are presented in Figure S24 in the SI. Selected bond distances and angles for both cations of **5** are listed in Table 4 (labeled as A and B). The structure features gold(I) ions bonded to two NHC ligands through the carbenic carbons. Each cation contains two copper(I) ions bonded to the pyridyl groups of the NHCs in a two-coordinate fashion. The copper(I) ions are canted toward the gold center, with Au−Cu distances ranging from 2.9762(5) to 3.0694(5) Å. Unlike the linear alignment of the $[AuCu_2]^{3+}$ core in **3**·2CH$_3$CN, the trimetallic core of **5** is considerably distorted, with Cu1−Au1−Cu2 and Cu3−Au2−Cu4 angles of 125.409(14) and 128.731(14)°, respectively. Likewise, the copper geometry deviates from linearity, with N−Cu−N angles ranging from 160.17(15) to 162.93(14)°. To accommodate this distortion, the NHC ligands twist to place two opposing pyridyl rings near the Cu−Au−Cu pocket, with the other two picolyl rings oriented away. This distortion is also manifested in the dihedral angles of 68.35 and 67.23° between the benzimidazole rings of the NHC ligands. The Cu−N distances are notably shorter than those found in **3**·2CH$_3$CN and range from 1.908(3) to 1.937(4) Å.

Serendipitously, crystallization with unpurified reagent-grade nitromethane produced trace amounts of orange-luminescent crystals of $[AuCu_2(benzim(CH_2py)_2)_2(NCCH_2CH_3)_2](PF_6)_3$ (**6**), as shown in Scheme 3. This material cocrystallizes with the solvent-free material described above. Crystallographic information is presented in Table 1, while selected bond distances and angles for **6** are listed in Table 5. As shown in Figure 6, the structure of **6** is remarkably similar to that of **3**·2CH$_3$CN except **6** contains one propionitrile solvent molecule coordinated to each copper center. Propionitrile is a common impurity in nitromethane.[32] The complex crystallizes in the triclinic space group $P\bar{1}$ with half of the molecule in the asymmetric unit. Similar to **3**·2CH$_3$CN, the gold(I) center in **6** is linearly bonded to two NHC ligands, with flanking three-coordinate copper(I) ions bonded to two pyridyl rings and one propionitrile molecule. The Au−Cu distances are long [Au1···Cu1 = 4.5861(7) Å] and similar to those found in **3**·2CH$_3$CN. The copper ions adopt trigonal-planar geometries, with varying N−Cu−N angles that sum nearly to 360° [N3−Cu1−N4A = 131.78(19)°, N3−Cu1−N5 = 109.9(2)°, and N5−Cu1−N3A = 118.2(2)°]. The Cu−N distances are intermediate to those of **3**·2CH$_3$CN and **5** and range from 1.969(5) to 1.980(6) Å.

DOI: 10.1021/acs.inorgchem.5b00821
Inorg. Chem. 2015, 54, 6900−6909

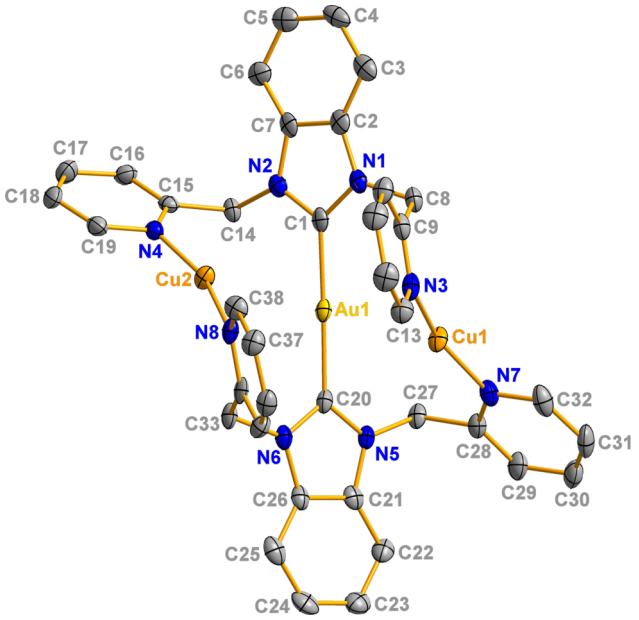

Figure 5. Thermal ellipsoid (50%) plot of the cationic portion of **5**. Hydrogen atoms are excluded for clarity. Two molecules of **5** appear in the asymmetric unit with similar bond parameters. Only one molecule is shown here, but both are included in Figure S24 in the SI.

Table 4. Selected Bond Distances (Å) and Angles (deg) for Cations A and B in 5

cation A		cation B	
Au1···Cu1	2.9762(5)	Au2···Cu3	3.0269(5)
Au1···Cu2	3.0694(5)	Au2···Cu4	3.0668(5)
Au1−C1	2.019(4)	Au2−C39	2.015(4)
Au1−C20	2.022(4)	Au2−C58	2.009(4)
Cu1−N3	1.936(4)	Cu3−N11	1.908(3)
Cu1−N7	1.937(4)	Cu3−N15	1.909(3)
Cu2−N4	1.925(3)	Cu4−N12	1.924(4)
Cu2−N8	1.923(3)	Cu4−N16	1.924(4)
Cu1−Au1−Cu2	125.409(14)	Cu3−Au2−Cu4	128.731(14)
C1−Au1−C20	178.61(16)	C39−Au2−C58	179.19(15)
N3−Cu1−N7	160.17(15)	N11−Cu3−N15	162.27(14)
N4−Cu2−N8	161.97(14)	N12−Cu4−N16	162.93(14)

Table 5. Selected Bond Distances (Å) and Angles (deg) for 6

Au1···Cu1	4.5861(7)	Cu1−Au1−Cu1A	180.0
Au1−C1	2.008(5)	N3−Cu1−N4A	131.78(19)
Cu1−N3	1.969(5)	N3−Cu1−N5	109.9(2)
Cu1−N4	1.971(5)	N5−Cu1−N3A	118.2(2)
Cu1−N5	1.980(6)		

In addition to their structural features, both **5** and **6** exhibit intense solid-state emissions distinct from those of **3**·2CH_3CN and **4**. Solid-state excitation and emission spectra of **5** and **6** are presented in Figure S25 in the SI. Crystals of **5** emit bright green (λ_{max} = 522 nm), while crystals of **6** are orange-emitters (λ_{max} = 573 nm). Additionally, compound **5** was further characterized by ^{1}H NMR spectroscopy. The ^{1}H NMR spectrum of **5** in CD_3NO_2 is nearly identical with those of **3**·2CH_3CN and **4** (Figure S26 in the SI). The only difference is the absence of the peak corresponding to acetonitrile in the spectrum of **5**. The spectrum features a singlet at 6.19 ppm

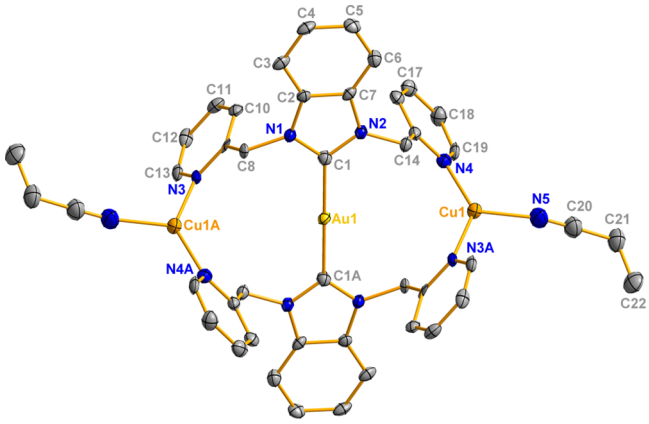

Figure 6. Thermal ellipsoid (50%) plot of the cationic portion of **6**. Hydrogen atoms are excluded for clarity. The atoms labeled with A are generated through inversion.

corresponding to the methylene protons and several multiplets ranging from 7.70 to 8.27 ppm. Furthest downfield, there is a singlet at 8.65 ppm corresponding to the protons closest to the nitrogen atoms of the pyridyl rings.

As shown in Scheme 2, both **3**·2CH_3CN and **4** exhibit remarkable luminescent mechanochromism, although the respective processes are slightly different. When **3**·2CH_3CN or **4** is ground in a mortar and pestle, the blue/aquamarine emission immediately becomes yellow (λ_{max} = 532 nm, *ground*-**4**), as shown in Figure 4. The addition of acetonitrile to *ground*-**4** reverses the process (Figure S27 in the SI), and after solvent evaporation, the deep-blue (λ_{max} = 461 nm) emission of the powder returns. The process is repeatable, and subsequent grinding regenerates the yellow emission. Photographs of **4**, *ground*-**4**, and *ground*-**4** after the addition of acetonitrile are presented in Figure 7. A video of the reversible luminescent mechanochromism process is included in the SI.

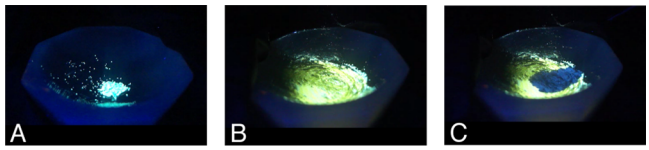

Figure 7. Photographs of powders of **4** (A), *ground*-**4** (B), and *ground*-**4** after the addition of acetonitrile (C) under UV light.

Heat also produces dramatic changes to the photoluminescence of solid samples of **3**·2CH_3CN or **4**. As shown in Scheme 2, heating samples of **3**·2CH_3CN past 150 °C produces a powder (**7**) with a muted yellow emission that is unique from the other complexes reported here (Figure S28 in the Supporting Information). This process is thermally irreversible, but upon recrystallization with acetonitrile, **3**·2CH_3CN is regenerated. Recrystallization from purified nitromethane and diethyl ether reproduces **5**. Thermolysis of **3**·2CH_3CN was followed by thermal gravimetric analysis (TGA; Figure S29 in the SI). At room temperature, the material begins to lose acetonitrile, and by ~62 °C, the complex has lost four of its six acetonitrile molecules. Further heating to ~158 °C eliminates the remaining two acetonitrile molecules to produce a solvent-free form. This material is compositionally identical with **5** (Figure 1) as determined by NMR spectroscopy. Aside from the loss of bands associated with acetonitrile,

DOI: 10.1021/acs.inorgchem.5b00821
Inorg. Chem. 2015, 54, 6900−6909

the ATR-IR spectrum of the heated material is not significantly different from that of the **4** or *ground*-**4** precursor.

The structural differences between **4** and *ground*-**4** are not easily determined. The ^{1}H NMR spectra of **4** and *ground*-**4** are nearly identical. Both spectra show the presence of two acetonitrile molecules and contain similar profiles for the ligand protons (Figure 1). Because of the nearly indistinguishable solution NMR spectra of **4** and *ground*-**4**, ^{19}F{^{1}H} and ^{31}P{^{1}H} solid-state NMR spectroscopy was used to characterize the powders. As shown in Figure S30 in the SI, the ^{31}P{^{1}H} and ^{19}F{^{1}H} solid-state NMR spectra of **4** and *ground*-**4** are identical, suggesting similar anion environments. The ATR-IR spectra do show subtle differences in the acetonitrile environments. Upon grinding, the broad band at 2273 cm^{-1} in **4** splits into two bands at 2268 and 2282 cm^{-1} associated with *ground*-**4** (Figure S20 in the SI). Furthermore, samples of **4**, *ground*-**4**, and **7** were also characterized by powder X-ray diffraction (Figure S31 in the SI). The powder X-ray diffraction patterns of **4**, *ground*-**4**, and **7** are all broad and featureless and appear amorphous.

DISCUSSION

The impetus behind this work was to explore the vapor-luminescent potential of the benzimidazole containing $[AuCu_2(benzim(CH_2py)_2)_2(NCCH_3)_4]^{3+}$, **3**·2CH$_3$CN. This complex is quite similar to the previously reported[29] imidazole analogue $[AuCu_2(im(CH_2py)_2)_2(NCCH_3)_4]^{3+}$, which was shown to respond dramatically to methanol vapor. Interestingly, in **3**·2CH$_3$CN, no such behavior was observed, nor was any methanol form of this complex obtained. Although the lack of solid/vapor reactivity is easily rationalized by differences in packing arrangements between crystalline **3**·2CH$_3$CN and its imidazole NHC analogue, the apparent lack of methanol coordination was surprising given the facile synthesis of $[AuCu_2(im(CH_2py)_2)_2(CH_3OH)_2]^{3+}$. The primary difference between these two complexes is the incorporation of the benzimidazole backbone on the NHC. One hypothesis is that this added ring structure introduces enough steric encumbrance between the methylene linkages and the C−H moieties next to the benzimidazole ring juncture to inhibit the twisted orientation of the picolyl groups that was observed in $[AuCu_2(im(CH_2py)_2)_2(CH_3OH)_2]^{3+}$. In this imidazole NHC complex, the copper(I) centers maintain very short (2.72 Å) separations with the gold(I) centers, and the absence of these metallophilic interactions in the benzimidazole analogue could influence the coordination chemistry at the copper centers.

The facile loss of acetonitrile in **3**·2CH$_3$CN is also noteworthy. As shown by TGA and ^{1}H NMR spectroscopy, four acetonitrile molecules are readily lost upon exposure to air, leading to the formation of **4**, or with grinding to *ground*-**4**. In **4**, the ν(CN) band is broad but close in energy to that of $[Cu(CH_3CN)_4]PF_6$, suggesting that the remaining two acetonitrile molecules are coordinated to the copper(I) centers. However, upon grinding, the ν(CN) band splits slightly, suggesting different nitrile environments, but the energy of these bands suggests continued coordination. The ν(CN) band of uncoordinated acetonitrile appears at 2253 cm^{-1}. With this in mind, the cationic portion of the structures of **4** and *ground*-**4** are probably more similar to that of the propionitrile-containing three-coordinate copper complex **6**. In fact, Singh and Gupta[33] reported a three-coordinate dipyridylacetonitrilecopper(I) complex whose ν(CN) band appears at 2286 cm^{-1}, close to that observed in **4** and *ground*-**4**. However, there is no requirement that both copper centers maintain the same coordination number. It is possible that one copper remains four-coordinate, as seen in **3**·2CH$_3$CN, while the other is only two-coordinate, as observed in **5**. Given the breadth of the ν(CN) peaks in the ATR-IR spectra, any assignments must be made cautiously.

All attempts to crystallize **4** or *ground*-**4** produced only the solvent-free **5** or, in the presence of trace propionitrile, **6**. Even spiking solutions of purified nitromethane with acetonitrile yielded **3**·2CH$_3$CN and not the acetonitrile analogue of **6**. The observation of two-, three-, and four-coordinate copper(I) in the same system is unusual but not unprecedented.[34,35] Although four-coordinate copper(I) complexes are ubiquitous,[36−39] two- and three-coordinate copper(I) complexes are also well represented in the literature.[40−48] Recent theoretical work[49] in simple $[Cu(NH_3)_n]^{+}$ complexes suggests that the two-coordinate copper geometry is slightly more stable than the three- and four-coordinate systems; however, the differences are quite small, and these calculations cannot precisely model solvation. It is likely that the rapid deligation observed in the work reported here is entropically driven. The role of the gold(I) ion in this process is not clear. As mentioned above, the methanol-containing complex $[AuCu_2(im(CH_2py)_2)_2(CH_3OH)_2]^{3+}$ has a very short Au−Cu separation of ∼2.72 Å, and it was originally postulated that formation of this presumably attractive metallophilic interaction contributes to stabilization of the copper−methanol complex. However, the propionitrile complex **6**, which contains trigonal-planar copper centers, maintains long and presumably repulsive Au^{I}−Cu^{I} separations of ∼4.6 Å, indicating that stabilization by gold is unnecessary. In fact, the shortest Au^{I}−Cu^{I} separation (∼3.0 Å) in the complexes reported here is found in the solvent-free form, **5**, where the copper centers are two-coordinate and slightly puckered toward the central gold atom. At 3.0 Å, it is unlikely there is significant stabilization present.

The absence of significant Au^{I}−Cu^{I} interactions suggests that modulation of the emission is likely related to perturbation of the environment around the cuprous centers. Theoretical studies by Sakaki and Tsukamoto on the imidazole-based $[AuCu_2(NHC)_2]^{3+}$ system indicate that the emission is heavily dependent on the coordination geometry around copper and the extent of any Au···Cu interactions.[50] In the imidazole-based analogue of **3**·2CH$_3$CN, the emission is based on a metal-to-ligand charge transfer, specifically Cu d to pyridyl π^* orbital. In the methanol form, the Au−Cu distance decreases, and copper adopts a three-coordinate geometry. In this structural motif, the emission is greatly perturbed; the nature of the emission is best described as a metal−metal (MM) transition due to the stronger Au−Cu interactions.

Desolvation of **3**·2CH$_3$CN to form acetonitrile-deficient **4** shifts the emission from blue (λ_{max} = 461 nm) to aquamarine (λ_{max} = 485 nm). Like the imidazole analogue, the emission change in **4** is likely due to a perturbation of the copper coordination geometry due to loss of coordinated solvent although without the formation of significant Au−Cu interactions. A dramatic mechanochromic emission change to bright yellow occurs when **3**·2CH$_3$CN or **4** is ground to form *ground*-**4** (λ_{max} = 532 nm). Solvent loss here is not a factor, and other than their unique emissions, **4** and *ground*-**4** are not easily distinguishable. The broad, featureless powder X-ray diffraction patterns of **4** and *ground*-**4** identify them both as amorphous solids rather than crystalline powders. The red shift of the emission in the formation of *ground*-**4** could be attributed to

DOI: 10.1021/acs.inorgchem.5b00821
Inorg. Chem. 2015, 54, 6900−6909

changes in acetonitrile ligation; however, subtle changes in complex–lattice or complex–anion interactions could also change the emission energy. We have recently reported that simple alteration of these interactions can lead to dramatic changes in the emission properties.[51] Likewise, because the degree of metal–metal interaction in *ground*-**4** is not known, perturbation of the copper centers by gold to red-shift the emission cannot be ruled out. This mechanism seems unlikely given that particularly short interactions are not observed in any of the complexes reported here. Of the compounds reported here, the emission of *ground*-**4** (λ_{max} = 532 nm) is closest in energy to that of **5** (λ_{max} = 522 nm; Figure S28 in the SI), which contains two-coordinate copper centers ~3.0 Å from gold with 2.6 Å contacts between the copper centers and a fluoride atom in the PF_6^- anion.

In addition to their mechanochromic properties, **3**·2CH_3CN and **4** exhibit luminescent thermochromism. Heating a sample of **3**·2CH_3CN or **4** produces an amorphous powder that is shown by NMR spectroscopy to be completely desolvated. This material is only weakly emissive in the visible spectrum, with a strong band near the UV. Although the thermochromic process is not reversible upon cooling, complex **3**·2CH_3CN or **5** is reproduced upon reconstitution of the heated material with acetonitrile or nitromethane, respectively. This lack of degradation suggests that the most reactive component of the complex, the NHC ligand, remains intact, while the new UV emission suggests a complex different from complexes **3**·2CH_3CN through **6**. It is possible that high temperature induces partial dissociation of the pyridyl groups from copper, which quenches the visible emission but generates a near-UV π–π^* similar to that of the ligand precursor.

Although there are several reports of mechanochromic gold(I) complexes, there are fewer examples featuring reversible mechanochromic processes, as was recently discussed in a review by Jobbágy and Deák.[25] The luminescent mechanochromism of **3**·2CH_3CN is an example of a crystalline-to-amorphous process that is reversible upon the addition of solvent. This is not an uncommon process and is seen in many luminescent mechanochromic transition-metal complexes. Likewise, there are several examples of mechanochromic transformations of gold(I) complexes, where the differences in emission are often attributed to differences in noncovalent interactions including aurophilic or metallophilic interactions.[25] However, manipulation of metallophilic interactions does not appear to be playing a role here. Rather, the changes in the optical properties are likely due to subtle changes in ligation about the cuprous centers. This observation suggests that other dipyridyl solvent complexes of copper(I) could undergo similar mechano- or thermoluminescent transformations. We are currently exploring this hypothesis in related NHC and phosphine systems.

CONCLUSION

Unlike the previously reported trimetallic gold(I)–copper(I) imidazole NHC complex, the analogous benzimidazolium complex **3** shows no vapochromic activity, nor does it react with methanol despite its structural similarity to the imidazole-based NHC complex. However, in this work we showed that the coordination environment around copper is easily perturbed either by simple exposure to air to produce an aquamarine-luminescent acetonitrile-deficient form or by grinding to produce a yellow emissive form. In all cases, the emission changes are reversible and appear to be related to coordination changes at the copper(I) centers driven by entropy with minimal perturbation by the gold(I) center. Two-, three-, and four-coordinate copper(I) complexes were characterized, and none contains particularly short MM separations. Last, heating complex **3**·2CH_3CN or **4** produces an acetonitrile-free species with a unique emission from the complexes reported here.

EXPERIMENTAL SECTION

The syntheses of 1-(pyridin-2-ylmethyl)-1*H*-benzimidazole,[52] 2-(chloromethyl)pyridine,[53] tetrahydrothiophenegold(I) chloride,[54] and $[Cu(NCCH_3)_4]PF_6$[55] are previously reported. All chemicals were used without further purification. Solution NMR spectra were recorded at 25 °C on Varian V500 and V400 NMR system spectrometers at the indicated frequencies and referenced to the residual solvent signals. Solid-state NMR spectra were recorded at 25 °C on a 500 MHz Bruker Avance Solids NMR spectrometer at the indicated frequency and referenced internally ($^{19}F\{^1H\}$ to $NaBF_4$ and $^{31}P\{^1H\}$ to KH_2PO_4). Excitation and emission (λ_{em} = 365 nm) spectra were recorded on a Jobin Yvon Horiba FluoroMax-3 spectrometer. Solution absorption spectra were recorded on a Shimadzu UV-2550 UV–vis spectrophotometer using 1 cm quartz cells. Solid-state absorption spectra were recorded on a Varian Cary 300 Bio UV–vis spectrophotometer equipped with a Labsphere DRA-CA-3300 integrating sphere. High-resolution ESI^+ MS spectra were recorded on a Agilent Technologies 6230 time-of-flight MS spectrometer. TGA was measured at a rate of 2 °C min^{-1} using a TA Instruments TGA Q50 analyzer. ATR-IR spectra were recorded at 4 cm^{-1} resolution on a Thermo Nicolet 6700 FT-IR instrument.

Single-crystal and powder X-ray diffraction was performed at 100 K on a Bruker SMART Apex II CCD instrument using graphite-monochromated Mo Kα radiation. The crystals and powders were covered in Paratone oil and mounted on glass fibers. Lorentz and polarization effects were corrected using *SAINT*,[56] and absorption corrections were applied using *SADABS*.[57] The crystal structures were solved using direct or Patterson methods using *OLEX2*.[58] The predicted powder pattern of **3**·2CH_3CN was obtained from the crystal structure using *Mercury 3.1*.[59]

Powders of **3**·2CH_3CN were ground with an agate mortar and pestle, and the conversion was monitored using a hand-held UV lamp. Drops of acetonitrile were added to the ground solid until a complete change in the emission was observed. The solvent was evaporated, and the grinding process was repeated until an emission change was again observed. Videos were recorded using a Sony CyberShot camera.

$[H(benzim(CH_2py)_2)_2]PF_6$. 1-(Pyridin-2-ylmethyl)-1*H*-benzimidazole (2.50 g, 11.9 mmol) and 2-(chloromethyl)pyridine (1.83 g, 14.3 mmol) were combined in a pressure tube with 40 mL of toluene. The suspension was heated at 140 °C for 8 h. The resulting precipitate was collected by filtration and washed with toluene. The crude solid was dissolved in water and filtered through Celite. An aqueous solution of NH_4PF_6 (9.74 g, 59.7 mmol) was added dropwise to the filtrate with stirring. A tan precipitate immediately formed and was filtered, washed with water, and dissolved in 100 mL of dichloromethane. The solution was dried using anhydrous magnesium sulfate and filtered through Celite. The solvent was removed under reduced pressure, affording the product as a tan solid in 74% yield (3.95 g, 8.84 mmol). ^1H NMR (500 MHz, $CDCl_3$): δ 9.53 (s, 1H), 8.51 (d, 2H), 7.82 (m, 2H), 7.76 (m, 2H), 7.60 (m, 2H), 7.57 (m, 2H), 7.29 (m, 2H), 5.75 (s, CH_2, 4H). $^{13}C\{^1H\}$ NMR (100 MHz, $CDCl_3$): δ 151.8, 150.0, 142.4, 138.0, 131.8, 127.5, 124.3, 123.5, 114.3, 52.9. MS (ESI^+). Calcd for $C_{19}H_{17}N_4^+$: m/z 301.14533 ($[M - PF_6]^+$). Found: m/z 301.14431.

$[Ag(benzim(CH_2py)_2)_2]PF_6$ (1). Ag_2O (40 mg, 0.172 mmol) and NaOH (1 M, 3 mL) were added to a solution of $[benzim(CH_2py)_2]$-PF_6 (300 mg, 0.673 mmol) and a catalytic amount of Bu_4NPF_6 in 30 mL of dichloromethane. The mixture was refluxed in the absence of light for 2.5 h. The solvent was removed by rotary evaporation, and the residue was dissolved in 20 mL of acetone. The mixture was filtered through Celite, and the filtrate was concentrated to 10 mL under vacuum. The product was precipitated with 30 mL of diethyl ether and isolated as a brown solid in 61% yield (175 mg, 0.205 mmol). ^1H

DOI: 10.1021/acs.inorgchem.5b00821
Inorg. Chem. 2015, 54, 6900–6909

NMR (500 MHz, $(CD_3)_2CO$): δ 8.47 (d, 4H), 7.80 (m, 4H), 7.73 (m, 4H), 7.51 (d, 4H), 7.44 (m, 4H), 7.28 (m, 4H), 5.97 (s, CH_2, 8H). $^{13}C\{^1H\}$ NMR (125 MHz, $(CD_3)_2CO$): δ 156.3, 150.6, 138.1, 135.0, 125.2, 124.2, 123.2, 113.2, 54.9. UV [CH_3CN; λ_{max}, nm (ε, M^{-1} cm^{-1})]: 256 (27000), 260 (28000), 266 (26000), 276 (21000), 282 (16000).

[Au(benzim(CH_2py)$_2$)$_2$]PF_6 (2). A 50 mL round-botttomed flask was charged with **1** (154 mg, 0.180 mmol) and Au(tht)Cl (49 mg, 0.211 mmol) in 50 mL of dichloromethane, and the mixture was stirred in the absence of light for 2 h. The solvent was removed by rotary evaporation, and the residue was dissolved in 20 mL of acetone. The mixture was filtered through Celite to remove AgCl, and the filtrate was concentrated to 5 mL under vacuum. The product was precipitated with 20 mL of diethyl ether and isolated as a tan solid in 66% yield (112 mg, 0.119 mmol). Crystals suitable for X-ray diffraction were grown from vapor diffusion of diethyl ether into an acetonitrile solution of **2**. ^1H NMR [500 MHz, $(CD_3)_2CO$]: δ 8.49 (d, 4H), 7.80 (m, 4H), 7.73 (m, 4H), 7.48 (m, 8H), 7.29 (m, 4H), 6.02 (s, 8H). $^{13}C\{^1H\}$ NMR [125 MHz, $(CD_3)_2CO$]: δ 192.4, 155.0, 149.7, 137.2, 133.8, 124.9, 123.3, 122.0, 112.6, 53.4. UV [CH_3CN; λ_{max}, nm (ε, M^{-1} cm^{-1})]: 255 (17000), 261 (18000), 266 (17000), 280 (15000), 290 (21000), 297 (17000). MS (ESI^+). Calcd for $C_{38}H_{32}AuN_8^+$: m/z 797.2410 ($[M - PF_6]^+$). Found: m/z 797.2404.

[$AuCu_2$(benzim(CH_2py)$_2$)$_2$($NCCH_3$)$_4$](PF_6)$_3$·2CH_3CN (3·2CH_3CN). A 50 mL round-botttomed flask was charged with **2** (312 mg, 0.348 mmol) and $[Cu(NCCH_3)_4]PF_6$ (256 mg, 0.689 mmol) in 30 mL of acetonitrile, and the mixture was stirred for 20 min. The solution was concentrated to 10 mL under vacuum. The product was precipitated with 20 mL of diethyl ether and isolated as a tan solid in 76% yield (435 mg, 0.264 mmol). Crystals suitable for X-ray diffraction were grown from vapor diffusion of diethyl ether into an acetonitrile solution of **3**·2CH_3CN. ^1H NMR (500 MHz, CD_3CN): δ 8.47 (d, 4H), 7.81 (m, 4H), 7.73 (m, 4H), 7.48 (m, 8H), 7.30 (m, 4H), 5.85 (s, 8H), 2.00 (s, 18H). $^{13}C\{^1H\}$ NMR (125 MHz, CD_3CN): δ 193.3, 155.8, 150.6, 138.3, 134.7, 126.0, 124.4, 122.9, 113.4, 54.3. UV [CH_3CN; λ_{max}, nm (ε, M^{-1} cm^{-1})]: 260 (49000), 268 (44000), 280 (45000), 288 (55000), 295 (46000). IR (ATR, cm^{-1}): 2279, 2253 [ν(CN)]. MS (ESI^+). Calcd for $C_{38}H_{32}AuCu_2N_8P_2F_{12}^+$: m/z 1213.0286 ($[M - (CH_3CN)_6 - PF_6]^+$). Found: m/z 1213.0282.

Compound 4. Powders of **3**·2CH_3CN were exposed to air for 2 h to form **4**. ^1H NMR (500 MHz, CD_3NO_2): δ 8.62 (d, 4H), 8.27 (t, 4H), 8.14 (m, 4H), 8.02 (m, 4H), 7.71 (m, 8H), 6.20 (s, 8H), 2.00 (s, 6H). $^{13}C\{^1H\}$ NMR (125 MHz, CD_3NO_2): δ 153.0, 151.0, 141.2, 133.5, 127.1, 126.3, 112.3, 54.5, 0.1. IR (ATR, cm^{-1}): 2271 [ν(CN)].

Compound *ground*-4. Crystals of **3**·2CH_3CN or powders of **4** were ground with an agate mortar and pestle until an emission change under UV light was observed to form *ground*-**4**. ^1H NMR (500 MHz, CD_3NO_2): δ 8.61 (d, 4H), 8.27 (t, 4H), 8.14 (m, 4H), 8.02 (m, 4H), 7.71 (m, 8H), 6.20 (s, 8H), 2.00 (s, 6H). $^{13}C\{^1H\}$ NMR (125 MHz, CD_3NO_2): δ 153.4, 151.3, 141.8, 133.5, 127.6, 126.4, 112.3, 54.9. IR (ATR, cm^{-1}): 2283, 2267 [ν(CN)].

Compound 5. Powders of **4** or *ground*-**4** were recrystallized by vapor diffusion of diethyl ether into a purified nitromethane solution to form **5**. ^1H NMR (500 MHz, CD_3NO_2): δ 8.65 (br, 4H), 8.27 (t, 4H), 8.13 (m, 4H), 8.01 (br, 4H), 7.70 (m, 8H), 6.19 (s, 8H).

Compound 7. Powders of **3**·2CH_3CN or **4** were heated to 150 °C and cooled to room temperature to form **7**. ^1H NMR (500 MHz, CD_3NO_2): δ 8.64 (br, 4H), 8.26 (br, 4H), 8.12 (br, 4H), 8.00 (br, 4H), 7.69 (br, 8H), 6.19 (s, 8H). $^{13}C\{^1H\}$ NMR (125 MHz, CD_3NO_2): δ 153.2, 151.3, 141.6, 133.6, 127.4, 126.3, 112.2, 54.7.

■ ASSOCIATED CONTENT

Supporting Information

X-ray crystallographic data for the complexes in CIF format, characterization of the compounds including NMR and optical spectra, video of grinding experiments, complete X-ray structural characterization including thermal ellipsoid plots, and tables of bond distances and angles. The Supporting Information is available free of charge on the ACS Publications website at DOI: 10.1021/acs.inorgchem.5b00821.

■ AUTHOR INFORMATION

Corresponding Author

*E-mail: vjc@unr.edu.

Notes

The authors declare no competing financial interest.

■ ACKNOWLEDGMENTS

The authors thank Dr. Stephen M. Spain for assistance with instrumentation.

■ REFERENCES

(1) Zhang, X.; Chi, Z.; Zhang, Y.; Liu, S.; Xu, J. *J. Mater. Chem. C* **2013**, *1*, 3376−3390.
(2) Chi, Z.; Zhang, X.; Xu, B.; Zhou, X.; Ma, C.; Zhang, Y.; Liu, S.; Xu, J. *Chem. Soc. Rev.* **2012**, *41*, 3878−3896.
(3) Caruso, M. M.; Davis, D. A.; Shen, Q.; Odom, S. A.; Sottos, N. R.; White, S. R.; Moore, J. S. *Chem. Rev.* **2009**, *109*, 5755−5798.
(4) Mizukami, S.; Houjou, H.; Sugaya, K.; Koyama, E.; Tokuhisa, H.; Sasaki, T.; Kanesato, M. *Chem. Mater.* **2005**, *17*, 50−56.
(5) Tzeng, B.-C.; Chang, T.-Y.; Sheu, H.-S. *Chem. - Eur. J.* **2010**, *16*, 9990−9993.
(6) Ito, H.; Saito, T.; Oshima, N.; Kitamura, N.; Ishizaka, S.; Hinatsu, Y.; Wakeshima, M.; Kato, M.; Tsuge, K.; Sawamura, M. *J. Am. Chem. Soc.* **2008**, *130*, 10044−10045.
(7) Seki, T.; Sakurada, K.; Ito, H. *Angew. Chem., Int. Ed.* **2013**, *52*, 12828−12832.
(8) Lasanta, T.; Olmos, M. E.; Laguna, A.; López-de-Luzuriaga, J. M.; Naumov, P. *J. Am. Chem. Soc.* **2011**, *133*, 16358−16361.
(9) Liang, J.; Hu, F.; Lv, X.; Chen, Z.; Chen, Z.; Yin, J.; Yu, G.-A.; Liu, S. H. *Dyes Pigm.* **2012**, *95*, 485−490.
(10) Osawa, M.; Kawata, I.; Igawa, S.; Hoshino, M.; Fukunaga, T.; Hashizume, D. *Chem. - Eur. J.* **2010**, *16*, 12114−12126.
(11) Abe, T.; Itakura, T.; Ikeda, N.; Shinozaki, K. *Dalton Trans.* **2009**, 711−715.
(12) Ni, J.; Zhang, X.; Wu, Y.-H.; Zhang, L.-Y.; Chen, Z.-N. *Chem. - Eur. J.* **2011**, *17*, 1171−1183.
(13) Ni, J.; Zhang, X.; Qiu, N.; Wu, Y.-H.; Zhang, L.-Y.; Zhang, J.; Chen, Z.-N. *Inorg. Chem.* **2011**, *50*, 9090−9096.
(14) Zhang, X.; Wang, J.-Y.; Ni, J.; Zhang, L.-Y.; Chen, Z.-N. *Inorg. Chem.* **2012**, *51*, 5569−5579.
(15) Choi, S. J.; Kuwabara, J.; Nishimura, Y.; Arai, T.; Kanbara, T. *Chem. Lett.* **2012**, *41*, 65−67.
(16) Kitani, N.; Kuwamura, N.; Tsukuda, T.; Yoshinari, N.; Konno, T. *Chem. Commun.* **2014**, *50*, 13529−13532.
(17) Tsukuda, T.; Kawase, M.; Dairiki, A.; Matsumoto, K.; Tsubomura, T. *Chem. Commun.* **2010**, *46*, 1905−1907.
(18) Babashkina, M. G.; Safin, D. A.; Bolte, M.; Garcia, Y. *Dalton Trans.* **2011**, *40*, 8523−8526.
(19) Perruchas, S.; Le Goff, X. F.; Maron, S.; Maurin, I.; Guillen, F.; Garcia, A.; Gacoin, T.; Boilot, J.-P. *J. Am. Chem. Soc.* **2010**, *132*, 10967−10969.
(20) Bi, H.; Chen, D.; Li, D.; Yuan, Y.; Xia, D.; Zhang, Z.; Zhang, H.; Wang, Y. *Chem. Commun.* **2011**, *47*, 4135−4137.
(21) Szerb, E. I.; Talarico, A. M.; Aiello, I.; Crispini, A.; Godbert, N.; Pucci, D.; Pugliese, T.; Ghedini, M. *Eur. J. Inorg. Chem.* **2010**, *2010*, 3270−3277.
(22) Shan, G.-G.; Li, H.-B.; Cao, H.-T.; Zhu, D.-X.; Li, P.; Su, Z.-M.; Liao, Y. *Chem. Commun.* **2012**, *48*, 2000−2002.
(23) Shan, G.-G.; Li, H.-B.; Zhu, D.-X.; Su, Z.-M.; Liao, Y. *J. Mater. Chem.* **2012**, *22*, 12736−12744.
(24) Mastropietro, T. F.; Yadav, Y. J.; Szerb, E. I.; Talarico, A. M.; Ghedini, M.; Crispini, A. *Dalton Trans.* **2012**, *41*, 8899−8907.
(25) Jobbágy, C.; Deák, A. *Eur. J. Inorg. Chem.* **2014**, *2014*, 4434−4449.

DOI: 10.1021/acs.inorgchem.5b00821
Inorg. Chem. 2015, 54, 6900−6909

(26) Seki, T.; Sakurada, K.; Muromoto, M.; Ito, H. *Chem. Sci.* **2015**, *6*, 1491−1497.
(27) Seki, T.; Ozaki, T.; Okura, T.; Asakura, K.; Sakon, A.; Uekusa, H.; Ito, H. *Chem. Sci.* **2015**, *6*, 2187−2195.
(28) Ito, H.; Muromoto, M.; Kurenuma, S.; Ishizaka, S.; Kitamura, N.; Sato, H.; Seki, T. *Nat. Commun.* **2013**, *4*, 2009.
(29) Strasser, C. E.; Catalano, V. J. *J. Am. Chem. Soc.* **2010**, *132*, 10009−10011.
(30) Zhang, X.; Gu, S.; Xia, Q.; Chen, W. *J. Organomet. Chem.* **2009**, *694*, 2359−2367.
(31) Lin, I. J.; Vasam, C. S. *Can. J. Chem.* **2005**, *83*, 812−825.
(32) Coetzee, J. F.; Chang, T.-H. *Pure Appl. Chem.* **1986**, *58*, 1541−1545.
(33) Singh, A. P.; Gupta, R. *Eur. J. Inorg. Chem.* **2010**, *2010*, 4546−4554.
(34) Lopez, S.; Keller, S. W. *Inorg. Chem.* **1999**, *38*, 1883−1888.
(35) Parsons, S.; Pikramenou, Z.; Solan, G. A.; Winpenny, R. E. P. *J. Cluster Sci.* **2000**, *11*, 227−232.
(36) Rodig, O. R.; Brueckner, T.; Hurlburt, B. K.; Schlatzer, R. K.; Venable, T. L.; Sinn, E. *J. Chem. Soc., Dalton Trans.* **1981**, 196−199.
(37) Amendola, V.; Boiocchi, M.; Brega, V.; Fabbrizzi, L.; Mosca, L. *Inorg. Chem.* **2010**, *49*, 997−1007.
(38) Karlin, K. D.; Dahlstrom, P. L.; Stanford, M. L.; Zubieta, J. *J. Chem. Soc., Chem. Commun.* **1979**, 465−467.
(39) Schindler, S.; Szalda, D. J.; Creutz, C. *Inorg. Chem.* **1992**, *31*, 2255−2264.
(40) Knaust, J. M.; Inman, C.; Keller, S. W. *Chem. Commun.* **2004**, 492−493.
(41) Karlin, K. D.; Gultneh, Y.; Hutchinson, J. P.; Zubieta, J. *J. Am. Chem. Soc.* **1982**, *104*, 5240−5242.
(42) Karlin, K. D.; Hayes, J. C.; Gultneh, Y.; Cruse, R. W.; McKown, J. W.; Hutchinson, J. P.; Zubieta, J. *J. Am. Chem. Soc.* **1984**, *106*, 2121−2128.
(43) Blake, A. J.; Hubberstey, P.; Li, W.-S.; Quinlan, D. J.; Russell, C. E.; Sampson, C. L. *J. Chem. Soc., Dalton Trans.* **1999**, 4261−4268.
(44) Beitat, A.; Foxon, S. P.; Brombach, C.-C.; Hausmann, H.; Heinemann, F. W.; Hampel, F.; Monkowius, U.; Hirtenlehner, C.; Knör, G.; Schindler, S. *Dalton Trans.* **2011**, *40*, 5090−5101.
(45) Krylova, V. A.; Djurovich, P. I.; Whited, M. T.; Thompson, M. E. *Chem. Commun.* **2010**, *46*, 6696−6698.
(46) Chan, W.-H.; Peng, S.-M.; Che, C.-M. *J. Chem. Soc., Dalton Trans.* **1998**, 2867−2872.
(47) Zhao, S.-B.; Wang, R.-Y.; Wang, S. *Inorg. Chem.* **2006**, *45*, 5830−5840.
(48) Pang, H.; Zhang, C.; Peng, J.; Wang, Y.; Sha, J.; Tian, A.; Zhang, P.; Chen, Y.; Zhu, M.; Su, Z. *Eur. J. Inorg. Chem.* **2009**, *2009*, 5175−5180.
(49) Pavelka, M.; Burda, J. V. *Chem. Phys.* **2005**, *312*, 193−204.
(50) Tsukamoto, S.; Sakaki, S. *Dalton Trans.* **2013**, *42*, 4809−4821.
(51) Chen, K.; Strasser, C. E.; Schmitt, J. C.; Shearer, J.; Catalano, V. J. *Inorg. Chem.* **2012**, *51*, 1207−1209.
(52) Guo, J.; He, P.; Yang, L.; Liu, X.; Lv, L.; Shi, Y.; Cao, C. *J. Chem. Res.* **2012**, *36*, 111−113.
(53) Iturrospe, A.; Artetxe, B.; Reinoso, S.; San Felices, L.; Vitoria, P.; Lezama, L.; Gutiérrez-Zorrilla, J. M. *Inorg. Chem.* **2013**, *52*, 3084−3093.
(54) Uson, R.; Laguna, A.; Laguna, M.; Briggs, D. A.; Murray, H. H.; Fackler, J. P. *Inorg. Synth.* **1989**, *26*, 85−91.
(55) Kubas, G. J. *Inorg. Synth.* **1990**, *28*, 68−70.
(56) *SAINT: Program for data reduction*, version 7.68A; Bruker AXS: Madison, WI, 2009.
(57) Sheldrick, G. M. *Acta Crystallogr., Sect. A: Found. Crystallogr.* **2008**, *64*, 112−122.
(58) Dolomanov, O. V.; Bourhis, L. J.; Gildea, R. J.; Howard, J. A. K.; Puschmann, H. *J. Appl. Crystallogr.* **2009**, *42*, 339−341.
(59) Macrae, C. F.; Bruno, I. J.; Chisholm, J. A.; Edgington, P. R.; McCabe, P.; Pidcock, E.; Rodriguez-Monge, L.; Taylor, R.; van de Streek, J.; Wood, P. A. *J. Appl. Crystallogr.* **2008**, *41*, 466−470.

DOI: 10.1021/acs.inorgchem.5b00821
Inorg. Chem. 2015, 54, 6900−6909